# Helix-Stabilizing Nonpolar Interactions between Tyrosine and Leucine in Aqueous and TFE Solutions: 2D-$^1$H NMR and CD Studies in Alanine-Lysine Peptides[†]

S. Padmanabhan,* M. A. Jiménez, D. V. Laurents, and M. Rico*

*Instituto de Estructura de la Materia, Consejo Superior de Investigaciones Cientificas, Madrid, Spain*

*Received June 9, 1998; Revised Manuscript Received October 7, 1998*

ABSTRACT: Interactions between side chains spaced ($i$, $i + 3$) and ($i$, $i + 4$) may explain the context dependence of helix propensities observed in different systems. Nonpolar residues with these spacings occur frequently in protein helices and stabilize isolated peptide helices. Here ($i$, $i + 3$) and ($i$, $i + 4$) nonpolar interactions between Tyr and Leu in different solution conditions are studied in detail in alanine-based peptides using 2D $^1$H NMR and CD spectroscopy. Helix contents analyzed using current models for helix-coil transitions yield interaction energies which demonstrate significant helix stabilization in aqueous 1 M NaCl solutions by Tyr-Leu or Leu-Tyr pairs when spaced ($i$, $i + 4$) and, to a smaller extent, when spaced ($i$, $i + 3$), comparable to those estimated for other residue pairs. The interactions persist in solutions containing TFE, a helix-stabilizing solvent believed to diminish hydrophobic interactions, but not in helix-destabilizing 6 M urea. $^1$H NMR resonances for all peptides and solution conditions except in 6 M urea were completely assigned. NMR data indicate that the N-terminal residues are more helical and that the *N*-acetyl group participates in helix formation. The two ($i$, $i + 4$) spaced pairs show the same pattern of NOE cross-peaks between the Tyr and Leu side chains, as do the two ($i$, $i + 3$) pairs in 1 M NaCl as well in TFE solutions, and correspond well with that expected for the specific Tyr-Leu pair with side-chain contacts in protein helices.

Helix propensities of amino acids examined in a number of different peptide and protein systems often show good correlations between the different systems, but sizable discrepancies exist in the magnitudes, ranges, and, sometimes, in the rank order of helix propensities, a context dependence that has been rationalized in terms of differing side-chain/side-chain interactions (*1*). Thus the differences between the earliest determinations of helix propensities in polymers based on hydroxylalkyl-L-glutamines (*2*) from those in the simplest alanine-rich peptides (*3*−*6*) could be rationalized in terms of side-chain interactions involving the bulky hydroxyalkyl moiety in the earlier studies (*7*). The importance of interactions between specific bulky amino acid residues which are spaced ($i$, $i + 3$) and ($i$, $i + 4$) in affecting the apparent helix propensities has been reiterated in several recent articles (*8*−*10*), as has their role in protein folding and stability (*11, 12*). Identifying and quantifying such interactions would therefore be of considerable value in studies on helix propensities and on protein folding, stability, and design.

Protein helices typically contain one or more ($i$, $i + 3$) or ($i$, $i + 4$) nonpolar amino acid pairs. Such nonpolar amino acid pairs can be involved in hydrophobic interactions, and their importance in protein folding and stability was proposed several years ago (*13*−*17*). However, the existence of sequence-specific interactions between nonpolar side chains to stabilize isolated helices was experimentally demonstrated only recently: they were first shown for Leu and X (X = Tyr, Phe, Val, Ile, Leu) and for Tyr and Val when spaced ($i$, $i + 4$) (*18, 19*) and then extended to include ($i$, $i + 4$) Phe-Met interactions (*20, 21*). These interactions have been examined in a statistical study of protein structures (*22*) and in theoretical calculations (*23*), but interaction energies explicitly determined from experimental data are available only for the helix-stabilizing ($i$, $i + 4$) Phe-Met nonpolar pair (*20, 21*) and for interactions between the nonpolar Trp and charged or uncharged His (*24*). This is because the classical helix-coil theories (*25, 26*) for analyzing experimental data were only very recently extended to include both end-capping and sequence-specific pairwise side-chain interactions (*6, 20, 27*−*30*). Furthermore, amino acid helix propensities in 40% trifluorethanol (TFE[1]) have now been determined (*6*). This allows quantitative evaluation of the effects of TFE on the energetics of side-chain interactions such as the hydrophobic interactions which occur between

[†] This work was supported by grant PB93-0189 from the Dirección General de Ciencia y Tecnología (Spain). D.V.L. is a postdoctoral fellow of the Leukemia Society of America.

* To whom correspondence should be addressed at Instituto de Estructura de la Materia-CSIC, Serrano 119, 28006 Madrid, Spain. E-mail: empadhu@rocky2.roca.csic.es; rico@malika.iem.csic.es. Fax: 34-91-564 2431.

[1] Abbreviations: 1D, one-dimensional; 2D, two-dimensional; CD, circular dichroism; COSY, scalar-coupled correlation spectroscopy; DQF−COSY, double quantum filtered correlation spectroscopy; ESR, electron spin resonance; Fmoc, 9-fluorenyl methoxycarbonyl; NMR, nuclear magnetic resonance; $^3J_{HN\alpha}$, amide proton-α-proton vicinal spin−spin coupling constant; mL-R, modified Lifson-Roig; NOESY, nuclear Overhauser enhancement and exchange spectrocopy; OPfp, pentafluorophenyl; ROESY, rotating frame exchange spectroscopy; SD, standard deviation; TFA, trifluoroacetic acid; TFE, trifluoroethanol; TOCSY, total correlation spectroscopy; TSP, 3-trimethyl-silyl(2,2′,3,3′-$^2H_4$)-propionate.

10.1021/bi9813678 CCC: $15.00 
Published on Web 11/13/1998

nonpolar residues. Such an evaluation is relevant because contributions to helix stability from hydrophobic interactions are believed to be weakened by the lower solvent polarity of solutions containing TFE, even though the helix contents increase with increasing TFE up to, but not beyond, 40 vol % (refs *6*, *31*−*36* and references therein).

In the present study, we use CD and 2D-$^1$H NMR spectroscopy to investigate in detail the ($i$, $i + 4$) and ($i$, $i + 3$) nonpolar interactions between Tyr and Leu in peptides based on the extensively used alanine-rich model peptide system (*3*−*7*, *18*−*20*). The peptides all with identical amino acid compositions differ only in the spacings and orientations of Tyr and Leu present in each one of them. They are twelve residues long, sufficient for helix formation with helix contents in the range suitable for quantitative analysis using current models for helix-coil transitions (see ref *6*). Problems associated with NMR spectral overlap caused by the presence of several alanines would also be expected to be less severe in these peptides which are shorter relative to the longer ones generally employed in most studies using this model peptide system (*3*−*7*, *18*−*21*). The interactions identified in aqueous 1 M NaCl solutions in the earlier report (*18*) are investigated in detail here using 2D-NMR methods and quantitated. In addition we examine if these Tyr-Leu interactions persist in helix-destabilizing 6 M urea solutions or in the presence of TFE. The ($i$, $i + 3$) and ($i$, $i + 4$) Tyr-Leu and Leu-Tyr interaction energies in aqueous 1 M NaCl solutions as well as in 40% TFE are estimated by analyzing the peptide helix contents using the currently available models and parameters for helix-coil transitions (*6*, *28*) and compared with those for some other nonpolar amino acid pairs. An important aim of the present study is to use 2D-$^1$H NMR spectroscopy to examine the nature of the peptide helices and of the contacts between their interacting Tyr and Leu side chains in the different solution conditions, and thereby, to infer the conformational basis for these interactions. Contacts between Tyr and Leu would be indicated by NOE cross-peaks between their side chains in a clean area of the 2D-NOESY spectrum since the aromatic Tyr, as opposed to Val or Ile, has side-chain proton NMR chemical shifts distinctly different from those of the Leu side chain. Tyr ring currents can also influence the side-chain proton chemical shifts of a proximal Leu. The contacts for a specific spacing and orientation of the Tyr and Leu pair in the peptides studied here as inferred from NMR data are compared with the contacts, side-chain conformations, and the side-chain NOEs observed for that pair in protein helices.

## EXPERIMENTAL PROCEDURES

*Peptide Synthesis.* Each peptide was synthesized in a separate fine mesh polypropylene bag (Propyltex fabric 74 mm, Tetko Inc. Chicago, IL) employing the multiple solid-phase synthesis procedure (*37*) on a 0.03−0.05 mmol scale with 0.1−0.15 g of a 0.49 meq/g polystyrene Fmoc resin (Novabiochem) and either the active ester coupling procedure using the OPfp esters of the Fmoc amino acids (Bachem) and HOBT (1-hydroxy-benzotriazole from Sigma), or using the Fmoc-amino acids activated by HOBT, PyBOP (benzotriazole-1-yl-oxy-tris-pyrrolidino-phosphonium hexafluorophosphate from Novabiochem), and *N*-methylpyrrolidinone (Sigma). Peptides were acetylated at the N-terminus using acetic anhydride and then cleaved from the resin by treatment with 95:5 TFA/anisole mixture for 2−4 h to yield the crude peptides amidated at the C-terminus. The peptides were purified on a preparative Vydac C18 reverse-phase column using water/acetonitrile (0.1% TFA) gradients and lyophilized. They were >95% pure on an analytical Vydac C18 reverse-phase HPLC column, and their identities were confirmed by matrix-assisted laser desorption−ionization mass spectrometry and by NMR. Peptide concentrations were determined from the absorbance at 275 nm of the single Tyr present in all peptides in 6 M guanidium hydrochloride using an extinction coefficient, $\epsilon_{275}$, of 1450 $M^{-1}$ $cm^{-1}$ (*38*).

*Circular Dichroism (CD).* CD measurements were performed in a Jasco-720 spectropolarimeter equipped with a Neslab control unit and calibrated with (+)-10-camphorsulfonic acid (*39*) in 1 mm path length cuvettes, 0.2 nm step size, and 4 s response time, and averaged over 6 scans. Mean molar residue ellipticities at 222 nm ($[\Theta]_{222}$ in deg $cm^2$ $dmol^{-1}$) were measured at 2 °C and pH 3.0 [1 mM sodium phosphate/citrate/borate buffer or phosphate buffer alone using peptide concentrations between 50 and 80 $\mu$M in (a) 1 M NaCl; (b) 40% volume TFE/0.5 M NaCl; (c) 6 M urea/0.5 M NaCl]. Helix contents were estimated as described by Rohl et al. (*6*) using $[\Theta]_{222}$ values of 640 deg $cm^2$ $dmol^{-1}$ for 0% helix, and −31875 and −34530 deg $cm^2$ $dmol^{-1}$ for a 100% helical 12-residue and for a 16-residue peptide, respectively. An approximate correction for the Tyr aromatic side-chain contribution to the observed $[\Theta]_{222}$ (*40*) was done as described earlier (*5*). The measured helix contents were analyzed using the most recent versions of the programs and the corresponding parameters implementing the modified Lifson-Roig (mL-R) helix-coil theory (*6*) and AGADIR (*29*) in both of which ($i$, $i + 3$) and ($i$, $i + 4$) side-chain interactions are incorporated. First the helix contents were calculated setting the ($i$, $i + 3$) or ($i$, $i + 4$) interaction energies to 0; then the interaction energies were varied until the calculated helix content values matched those experimentally obtained. Errors in the interaction energies were obtained from those required by the helix-coil models to yield helix contents greater or less than the experimental value by 3%, the error in CD measurements.

*NMR Spectroscopy.* NMR data were collected in a Bruker AMX-600 NMR spectrometer with a $^1$H frequency of 600.13 MHz using 5 mm diameter NMR tubes. The spectra were acquired at 2 °C with samples at pH 3.0. NMR samples were prepared by dissolving lyophilized peptide in a 9:1 $H_2O$/$^2H_2O$ solution of 1 M NaCl, 1 mM sodium dihydrogen phosphate, and sodium TSP as the internal chemical shift reference. The aqueous NMR sample was diluted with deuterated TFE (TFE-$d_3$) to 40% TFE or lyophilized and dissolved in 6 M urea for measurements in TFE and 6 M urea, respectively. For measurements in 100% TFE, lyophilized peptide was dissolved in 100% TFE-$d_3$ containing NaCl and buffer to the extent soluble and the pH was adjusted to 3.0. 1D spectra were obtained using 16 K data points and 6000 Hz spectral width and averaged over 16 scans. The same spectral width and a 1 s recycle delay were used to acquire 2D spectra in the phase-sensitive mode using time-proportional phase incrementation (TPPI) technique (*41*) and presaturation of the water signal. Standard phase-cycling sequences and a data acquisition matrix size of 2048 × 512 ($t_2$ and $t_1$, respectively) were used for COSY (*42*), NOESY (*43*), and ROESY (*44*) spectra, with NOESY mixing times

Table 1: Peptides Sequences and CD Data

| peptide | sequence | Y−L/L−Y spacing | $[\Theta]_{222}$ (deg cm$^2$ dmol$^{-1}$)[a] | | |
|---|---|---|---|---|---|
| | | | 1 M NaCl | 40% TFE | 6 M urea |
| 3Y7L | Ac-AA**Y** KAA**L** AKAAA-$NH_2$ | ($i$, $i+4$) | −11000 | −24000 | 800 |
| 3Y6L | Ac-AA**Y** KA**L** AAKAAA-$NH_2$ | ($i$, $i+3$) | −6500 | −22200 | 1000 |
| 3YA | Ac-AA**Y** KAAAAKAAA-$NH_2$ | | −7900 | −26500 | 500 |
| 6L10Y | Ac-AAAKA **L** AAK**Y** AA-$NH_2$ | ($i$, $i+4$) | −14000 | −25200 | 800 |
| 7L10Y | Ac-AAAKAA **L** AK**Y** AA-$NH_2$ | ($i$, $i+3$) | −10700 | −23000 | 900 |
| 10YA | Ac-AAAKAAAAK**Y** AA-$NH_2$ | | −10200 | −23200 | 1000 |

[a] Mean residue ellipticity (error ±3%) for 50−80 $\mu$M peptide at 2 °C, pH 3.0.

of 200 and 150 ms and ROESY mixing times of 150 and 120 ms in aqueous and 40% TFE/water solutions, respectively. A data acquisition size of 4096 × 512 ($t_2 \times t_1$) was used for DQF−COSY (*45*) and for TOCSY spectra (mixing time 80 ms), the latter recorded using the standard MLEV17 spinlock sequence (*46*). The number of scans was 8 or 16 for the COSY and TOCSY experiments and 48 scans for the NOESY and ROESY experiments. Data were zero-filled, multiplied using a phase-shifted square-sine bell window function optimized for every spectrum, and processed using the Bruker UXNMR software. $^1$H resonances were assigned using standard assignment procedures (*47*). $^3J_{HN\alpha}$ coupling constants for nonoverlapping signals were determined using 1D spectra with high S/N and digital resolution where possible, by analyzing TOCSY spectra using the method of Stonehouse and Keeler (*48*) and from the separations between antiphase absorptive and dispersive peak extrema in DQF−COSY analyzed as described by Kim and Prestegard (*49*). The observed C$^\alpha$H proton chemical shifts of each residue and their respective random coil values (*50, 51*) were used to compute the chemical shift index or CSI (the difference between the observed and random coil chemical shifts of the C$^\alpha$H proton for each residue, refs *52, 53*) in aqueous and TFE solutions. Helix populations were also estimated from C$^\alpha$H shifts as described (*54, 55*). Cross-peaks in the 150 ms mixing time NOESY spectra of the peptides in 40% TFE were classified by visual inspection into strong, medium, and weak NOEs corresponding to upper limit distance constraints of <0.35, <0.45, and <0.55 nm, respectively. These, after appropriate pseudoatom corrections and the application of $\phi$ angle constraints for residues with $^3J_{HN\alpha} \leq$ 5 Hz in the range for $\alpha$ and $3_{10}$ helices, were used in structure calculations using the distance geometry program DIANA (*56*).

*Protein Database Analysis.* Sequence and conformational searches were done using the SCAN3D option of the program WHATIF (*57, 58*). This program uses a protein database of 315 nonhomologous proteins (sequence identity <25%) and a secondary structure assignment for each amino acid based on the program DSSP (*59*). The individual $\alpha$ and $3_{10}$ helical probabilities (0.034 and 0.039, respectively, for Tyr, and 0.106 and 0.074, respectively, for Leu) correspond to the ratios of helical Tyr ($\alpha$ = 665, $3_{10}$ = 102) or Leu ($\alpha$ = 2083, $3_{10}$ = 196) to the total number of helical residues ($\alpha$ = 19 728; $3_{10}$ = 2634) in the database. The probability of finding two given residues at any two positions (=0.003 for Y−L or L−Y pairs, the product of their individual probabilities) multiplied by (i) the total number of helical five residue segments ($\alpha\alpha\alpha\alpha\alpha$ = 12 437; $3_{10}\alpha\alpha\alpha\alpha$ = 81) gives the expected number of ($i$, $i+4$) Y−L or L−Y pairs in the database; or (ii) four helical segments ($\alpha\alpha\alpha\alpha$ = 14 259; $3_{10}\alpha\alpha\alpha$ = 81) gives the expected number of ($i$, $i+3$) Y−L or L−Y pairs in the database. Each helical ($i$, $i+3$) or ($i$, $i+4$) Y−L or L−Y pair in the database identified in this manner was analyzed for dihedral angles, hydrophobic contacts, and possible NOE distances using the program NAOMI (*60*). In this method a sphere of diameter 4.5 Å is used to represent each side-chain carbon atom and its covalently bonded hydrogen(s). Interpenetration of two such spheres, one for each residue (Tyr and Leu here), is used to infer a hydrophobic contact between the two residues.

## RESULTS

*CD Data.* Table 1 lists the 12-residue peptides studied here, their sequences, and their mean molar residue ellipticities at 222 nm ($[\Theta]_{222}$ in deg cm$^2$ dmol$^{-1}$) in different solution conditions. Peptides 3Y7L, 3Y6L, 6L10Y, and 7L10Y have an ($i$, $i+3$) or ($i$, $i+4$) Y−L while peptides 3YA and 10YA contain no Leu. The peptides are all soluble in aqueous solutions and are monomeric as shown by the independence of $[\Theta]_{222}$ over a 10-fold change of concentration. This has also been experimentally demonstrated earlier for such alanine-based peptides (*4, 18*). In aqueous 1 M NaCl solutions at pH 3.0 and 2 °C the $[\Theta]_{222}$ values confirm that an ($i$, $i+4$) spacing is significantly helix-stabilizing relative to an ($i$, $i+3$) spacing for both Y−L and L−Y orientations: 3Y7L > 3Y6L, and 6L10Y > 7L10Y in helix content, as reported previously at pH 7.0 and 0 °C (*18*). Thus the small difference in temperature (0 to 2 °C) or the larger difference in pH (7.0 to 3.0) has little or no effect on helix content. Indeed $[\Theta]_{222}$ values for alanine-lysine peptides have been shown to be independent of pH in the range 3.0−7.0 (*3*). This is expected since the only titratable groups in these peptides, the side-chain Tyr OH and Lys $NH_2$ groups, have p$K_a \gg 7$. The lower pH of 3.0 was used in this study to reduce solvent exchange broadening of the amide proton NMR signals. $[\Theta]_{222}$ values for 3YA and 10YA reflect the combined effects of the absence of any Y−L or L−Y interaction and the replacement of Leu by the significantly more helix-stabilizing Ala (*6*). Evaluating the relative contributions from each of these factors requires analysis using models for helix-coil transitions described subsequently. For all the peptides, $[\Theta]_{222}$ values in 6 M urea are those expected for the absence of any defined structure, while $[\Theta]_{222}$ values in 40% (by volume) TFE/water solutions indicate helix contents significantly enhanced over those measured in the absence of TFE (Table 1). $[\Theta]_{222}$ and, therefore, the helix content for the ($i$, $i+4$) spaced Y−L or L−Y pair is greater (and outside of experimental error) than for the corresponding ($i$, $i+3$) spaced pair in 40% TFE, though the differences appear to be much smaller than in water solutions (Table 1), suggesting that helix stabilization

by ($i$, $i + 4$) spaced Y−L or L−Y pairs may persist to some extent in TFE solutions.

For each peptide in 1 M NaCl and in 40% TFE solutions, the helix content determined from $[\Theta]_{222}$ was analyzed in terms of the modified Lifson-Roig (mL-R) helix-coil theory (*6*) and AGADIR (*29*) to quantify the Y−L or L−Y interaction energies, as described in Experimental Procedures. Table 2 lists the observed helix contents, those predicted by the two models when neither the ($i$, $i + 3$) nor the ($i$, $i + 4$) side-chain interaction is included in the analysis, and the free energies of interaction ($\Delta G_{L-Y}$ in kcal mol$^{-1}$) required in each model to predict the observed helix contents. The error in $\Delta G_{L-Y}$ listed in Table 2 is the larger of the difference between the $\Delta G_{L-Y}$ calculated using the measured helix content and for that above or below this value by 3% (the experimental error in $[\Theta]_{222}$). Helix contents obtained after correcting the measured $[\Theta]_{222}$ for the Tyr aromatic side-chain contribution (*40*) which is assumed to be linearly related to the helix content (as done elsewhere, refs *5*, *24*) and the corresponding $\Delta G_{L-Y}$ are listed parenthetically in Table 2. It must be emphasized that this correction is approximate and that the dependences of the aromatic contribution on helix content, helix length, and sequence position and orientation of the aromatic group are not known. Since the Tyr contribution to $[\Theta]_{222}$ is positive (*40*), the observed, uncorrected $[\Theta]_{222}$ provides a lower limit value for the helix content and so for the corresponding $\Delta G_{L-Y}$.

Both mL-R and AGADIR models yield similar $\Delta G_{L-Y}$ in aqueous 1 M NaCl solutions (Table 2) and indicate that (a) ($i$, $i + 4$) and ($i$, $i + 3$) spaced Y−L or L−Y pairs are helix-stabilizing, the ($i$, $i + 4$) pair being more favorable than the ($i$, $i + 3$) pair in both the N- to C-terminal orientations of Tyr and Leu; (b) the L−Y orientation is more favorable than Y−L for a given spacing. The two models predict helix contents for the peptides 3YA and 10YA without a Leu which agree, within the experimental error, with those observed. Moreover, $\Delta G_{L-Y}$ values from the mL-R algorithm predict helix contents to within 3% of the measured values for some longer alanine-based peptides having ($i$, $i + 3$) or ($i$, $i + 4$) spaced Tyr and Leu and whose measured helix contents approach 75% (*18*), while the corresponding predictions using AGADIR are, in some cases, outside of this error (data not shown). The discrepancy between the two models may be the consequence of the different model assumptions and/or parameter values, as well as the uncertainties associated with applying either model as helix contents approach values ≥75% or <20% (*6*, *29*). CD data in 40% TFE were analyzed using the mL-R model alone since the necessary helix-coil parameters for this solution condition are available only for this model (*6*). Helix contents corrected for the aromatic contribution or those used in determining errors in $\Delta G_{L-Y}$ are too high in 40% TFE for analysis using the mL-R model as mentioned before (*6*). So the model could only be applied with the helix contents uncorrected for the Tyr aromatic contribution to obtain lower limit estimates for $\Delta G_{L-Y}$ (Table 2). Even these can have large uncertainties associated with them because the uncorrected helix contents also approach values close to 75% (*6*), but they do appear to suggest that helix stabilization by Tyr-Leu interactions persists to a small extent in 40% TFE at least for the ($i$, $i + 4$) spaced pairs.

Table 2: Analysis of CD Data of Tyr-Leu Peptides using the Modified Lifson-Roig (mL-R) and AGADIR Models[a]

| | 1 M NaCl | | | | | 40% TFE | | |
|---|---|---|---|---|---|---|---|---|
| | mL-R | | | AGADIR | | mL-R | | |
| peptide | % helix (measured)[b] | % helix expected for $\Delta G_{L-Y} = 0$ | $\Delta G_{L-Y}$ (kcal mol$^{-1}$) | % helix expected for $\Delta G_{L-Y} = 0$ | $\Delta G_{L-Y}$ (kcal mol$^{-1}$) | % helix (measured)[b] | % helix expected for $\Delta G_{L-Y} = 0$ | $\Delta G_{L-Y}$ (kcal mol$^{-1}$)[c] |
| 3Y7L | 36 (40) | 18 | −0.79 ± 0.10 (−0.91 ± 0.09) | 15 | −0.68 ± 0.08 (−0.80 ± 0.10) | 76 (85) | 74 | −0.12 |
| 3Y6L | 22 (25) | 19 | −0.24 ± 0.17 (−0.38 ± 0.14) | 17 | −0.32 ± 0.12 (−0.43 ± 0.11) | 70 (79) | 74 | 0.00 |
| 3YA | 26 (29) | 27 | | 25 | | 83 (93) | 92 | |
| 6L10Y | 45 (51) | 19 | −1.00 ± 0.09 (−1.17 ± 0.10) | 18 | −1.10 ± 0.08 (−1.27 ± 0.10) | 79 (89) | 74 | −0.32 |
| 7L10Y | 35 (39) | 20 | −0.62 ± 0.11 (−0.82 ± 0.10) | 23 | −0.57 ± 0.10 (−0.70 ± 0.10) | 73 (82) | 73 | 0.00 |
| 10YA | 33 (37) | 29 | | 30 | | 73 (83) | 93 | |

[a] Model calculations and error estimates as described in Experimental Procedures. [b] Values in brackets are those obtained using the correction for the Tyr aromatic contribution to far UV-CD as described in the text. [c] Errors and $\Delta G_{L-Y}$ for helix contents corrected for aromatic contribution are not estimated because of very high helix contents (see text).

Table 3: Effects of ($i$, $i + 3$) K−L or L−K Interactions on Helix Content

| | | | % helix[b] | | | | |
|---|---|---|---|---|---|---|---|
| | | | 1 M NaCl | | | 40% TFE | |
| peptide[a] | K−L spacing | L−K spacing | expt | mL-R[c] | AGADIR[c] | expt | mL-R |
| 3L | | ($i$, $i + 2$), ($i$, $i + 7$) | 43 | 44 | 35 | 75 | 78 |
| 7L | ($i$, $i + 2$) | ($i$, $i + 3$) | 45 | 42 | 39 | 78 | 78 |
| 8L | ($i$, $i + 3$) | ($i$, $i + 2$) | 44 | 42 | 42 | 73 | 78 |
| 12L | ($i$, $i + 7$), ($i$, $i + 2$) | | 44 | 45 | 41 | 72 | 77 |

[a] Peptide sequences are 3L, Ac-AA**L**A**K**AAAA**K**AAAGGY-$NH_2$; 7L, Ac-AAAA**K**A**L**AA**K**AAAGGY-$NH_2$; 8L, Ac-AAAA**K**AA**L**A**K**AAAGGY-$NH_2$; and 10L, Ac-AAAA**K**AAAA**K**A**L**AGGY-$NH_2$. [b] Experimental helix contents (error ± 4%) in columns labeled "expt" were calculated from $[\Theta]_{222}$ for 25−80 $\mu$M peptide at 2 °C, pH 3.0, while columns mL-R and AGADIR list the helix contents expected for no interactions between Lys and Leu as calculated using the respective model algorithm (see text).

*Tests for the Effects of* ($i$, $i + 3$) *K−L or L−K Interactions on Helix Content.* In a helical conformation, two bulky amino acid side chains can interact with one another when spaced ($i$, $i + 3$) or ($i$, $i + 4$) where they are on the same face of the helix, but not for other spacings such as (i, i+1) or (i, i+2) (*7*, *18*, *19*). In each of the 12-residue peptides examined above which contains an ($i$, $i + 3$) or ($i$, $i + 4$) Y−L or L−Y pair, an ($i$, $i + 3$) K−L or L−K pair is also present, so that the Leu and Lys side chains may also interact with one another. To test if this is the case and, if so, how it affects helix formation, four 16-residue peptides were examined by CD (Table 3). These peptides, relative to those with twelve residues described earlier, have an additional N-terminal Ala, and the Tyr, present solely for peptide concentration determination, is separated from the rest of the sequence by the flexible Gly-Gly linker to avoid any contribution from Tyr both to side-chain interactions and to $[\Theta]_{222}$ (*40*). Peptide 7L has an (i, i+2) K−L pair and an ($i$, $i + 3$) L−K pair as in peptides 3Y6L and 6L10Y, while peptide 8L has an ($i$, $i + 3$) K−L pair and an (i, i+2) L−K pair as in peptides 3Y7L and 7L10Y, with side-chain interactions possible only for the ($i$, $i + 3$) pair. 3L and 12L are control peptides having no ($i$, $i + 3$) or ($i$, $i + 4$) K−L or L−K pair. All four peptides are water-soluble and monomeric in aqueous solutions with $[\Theta]_{222}$ independent of concentration over a 10-fold range. In 1 M NaCl and in 40% TFE solutions, the four peptides have helix contents which agree very well with those predicted by the mL-R logarithm where no interactions between Lys and Leu are considered, suggesting that such interactions are absent or negligible. There is a lower degree correspondence with the values predicted by AGADIR for these peptides in 1 M NaCl solutions. These differences may again be a consequence of the differences in the two models and have been discussed before (*29*).

*NMR Assignments and Helical Structure in Aqueous 1 M NaCl and 40% TFE.* 2D-$^1$H NMR spectra of the 12-residue peptides containing Y−L or L−Y pairs show sufficiently good spectral dispersion in aqueous 1 M NaCl or 40% TFE solutions and permit a complete assignment using the standard strategy of identifying spin systems from COSY and TOCSY spectra followed by sequential assignments from NOESY and ROESY spectra (*47*). In 6 M urea the acetyl, Tyr, Leu, and the two Lys were assigned, but only a range of chemical shifts could be obtained for the majority of Ala residues because of considerable spectral overlap. ($^1$H NMR assignments are listed in tables in the Supporting Information). The increase in signal dispersion with increasing helix content is illustrated in Figure 1 which shows 2D NOESY spectra (pH 3.0/ 2 °C) for peptides 3Y6L and 6L10Y which have the lowest and highest helix contents, respectively, in aqueous 1 M NaCl, and considerably higher helix contents in 40% TFE. NOESY and ROESY spectra yield identical cross-peak patterns confirming the absence of spin-diffusion contributions. This is also consistent with the results of numerous other NMR studies using similar mixing times with peptides of similar lengths. The helical nature of individual residues for each peptide and solution condition can be inferred from sequential and medium-range NOEs, $^3J_{HN\alpha}$ coupling constants (*47*), and upfield shifts of α-CH resonances relative to random coil values (*52*, *53*). Another good probe for helical residues, the exchange of each amide proton with solvent, was not attempted because it requires $^{15}$N-labeling with alanine-based peptides (*61*); however the total amide proton exchange behavior is qualitatively consistent with CD data (*18*).

Figure 2 summarizes for each peptide examined by NMR the observed NOE connectivities in 1 M NaCl and 40% TFE aqueous solutions qualitatively classified as strong, medium, or weak. The number of sequential and medium-range NOEs (Figures 1 and 2) is a maximum in 40% TFE, is the least in 6 M urea, and parallels the rank order of helix contents (6L10Y > 3Y7L > 7L10Y > 3Y6L) in aqueous 1 M NaCl solutions. Some of these characteristic NOEs may simply be undetected because of signal overlap rather than be actually absent, but in general, the number of NOEs detected appears to increase with helix content and the accompanying improvement in spectral dispersion. Sequential αN ($i$, $i + 1$) NOEs are observed for all peptides and solution conditions, while NN($i$, $i + 1$) NOEs are maximum in number in 40% TFE but essentially absent in 6 M urea (Figure 2). A series of NN($i$, $i + 1$) NOEs suggests structures with dihedral angles in the α region of ($\phi$, $\psi$) space (*62*) but is not sufficient to confirm helical structure. This is best indicated by the presence of nonsequential, medium-range NOEs. In the peptides studied here, αN($i$, $i + 2$) NOEs, when observed, are generally associated with residues at or close to the N- and C-termini and may reflect a partial helical nature in these terminal regions (*62*), a conformational behavior also seen at the ends of protein helices (*63*−*65*). In 1 M NaCl aqueous solutions, we identified two αN($i$, $i + 4$) NOEs for peptide 3Y7L, one involving the acetyl group for peptides 7L10Y and 6L10Y, and none for peptide 3Y6L whose helix content by CD is the least (Figure 2). The presence of αN($i$, $i + 4$) and strong $\alpha\beta$($i$, $i + 3$) NOEs indicates that a significant population of the peptides is in α-helical conformations in 1 M NaCl aqueous solutions (*47*). In addition to αN($i$, $i + 3$) and $\alpha\beta$($i$, $i + 3$) NOEs, the maximum number of αN($i$, $i + 4$) NOEs and, consequently, the highest population of

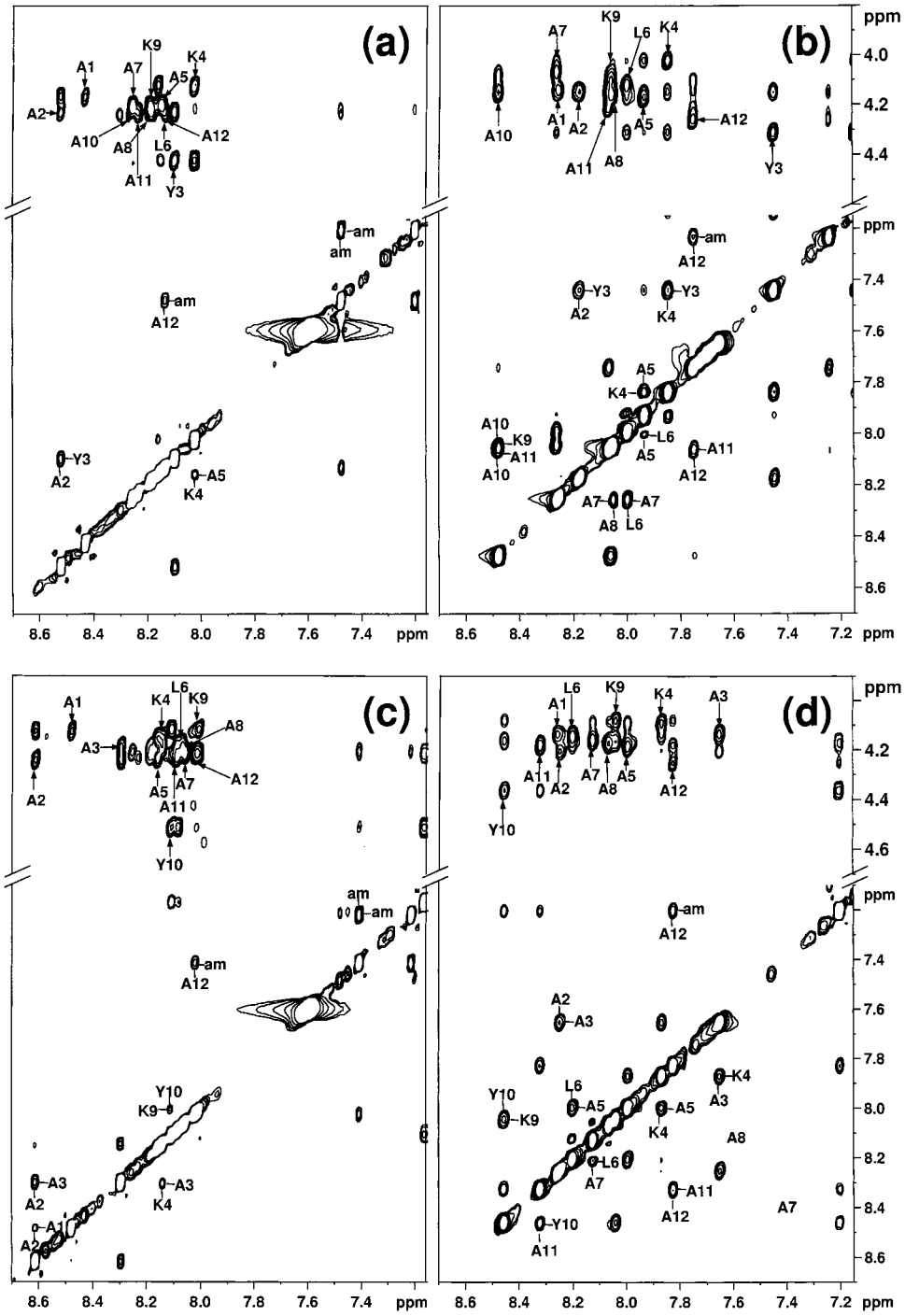


FIGURE 1: Representative 2D NOESY spectra at pH 3.0 and 2 °C of peptides: (a) 3Y6L in aqueous 1 M NaCl; (b) 3Y6L in 40% TFE; (c) 6L10Y in aqueous 1 M NaCl; and (d) 6L10Y in 40% TFE. Mixing times for the NOESY experiments are 200 ms in aqueous 1 M NaCl and 150 ms in 40% TFE. Intramolecular NH−C$^{\alpha}$H (indicated by arrows) and sequential NN(i, i+1) cross-peaks are shown.

α-helices is seen in 40% TFE. In general, significantly more ($i$, $i + 3$) and ($i$, $i + 4$) αN and α$\beta$ NOEs are observed at the N- than at the C-terminus, suggesting that the N-terminal residues are more helical. Moreover, in all the peptides, strong to medium ($i$, $i + 2$) and ($i$, $i + 3$) NOEs and medium to weak ($i$, $i + 4$) NOEs involving the *N*-acetyl $CH_3$ proton show its participation in helix formation.

The C$^{\alpha}$H−NH coupling constant, $^3J_{HN\alpha}$, for each residue is related to the backbone dihedral angle $\phi$, a stretch of at least three successive residues with $^3J_{HN\alpha} < 6.0$ Hz being characteristic of a helix (*47*). [$^3J_{HN\alpha} \approx 4.8$, 5.6, and 8.5 Hz, respectively, for α-helical, $3_{10}$-helical, and extended $\beta$-sheet residues in a recent comparison of $\phi$ angles in protein crystal structures and the corresponding $^3J_{HN\alpha}$ determined by NMR (*66*)]. In this study, $^3J_{HN\alpha}$ values were estimated by analyzing 2D NMR spectra and checked where possible with those from 1D spectra with high digital resolution (see Experimental Procedures). They are used only qualitatively to infer helicity (Figure 2) because they can vary by as much as 1−1.5 Hz (close to the digital resolution in the 2D experiments) and reflect an ensemble average. In both 1 M NaCl and 40% TFE solutions, $^3J_{HN\alpha}$ where measurable are, in general, ≤5 Hz for the N-terminal and central residues, but ≥6 Hz for the C-terminal residues, thus indicating that the

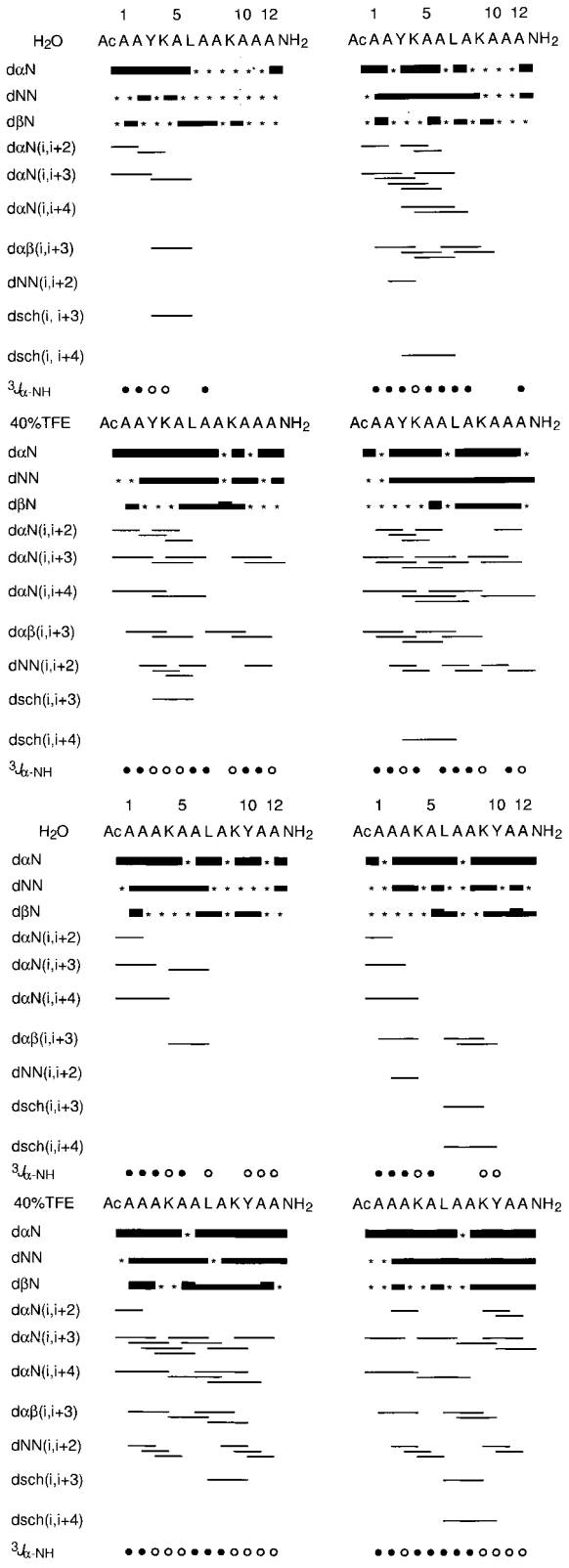


FIGURE 2: Summary of NMR data for the peptides in aqueous 1 M NaCl and 40% TFE solutions at pH 3.0 and 2 °C. For residues $i$, $i + 2$, $i + 3$, and $i + 4$ the sequential, $C^{\alpha}H-NH$ ($d_{\alpha N}$), NH−NH ($d_{NN}$), and $C^{\beta}H-NH$ ($d_{\beta N}$) NOE, the medium range, $C^{\alpha}H-NH$ ($d_{\alpha N}$-($i$, $i + 2$), $d_{\alpha N}$($i$, $i + 3$), $d_{\alpha N}$($i$, $i + 4$)), $C^{\alpha}H-C^{\beta}H$ ($d_{\alpha\beta}$($i$, $i + 3$)), and NH−NH ($d_{NN}$ ($i$, $i + 2$)), and side-chain/side-chain ($d_{sch}$($i$, $i + 3$), $d_{sch}$($i$, $i + 4$)) NOE connectivities are shown with the thick, medium, and thin bars indicating strong, medium, and weak NOE connectivities. $^3J_{HN\alpha}$ is the amide-αCH proton−proton vicinal spin−spin coupling constant with closed circles for $^3J_{HN\alpha} \leq 5$ Hz and open circles for $^3J_{HN\alpha} \geq 6$ Hz.

N-terminal residues are more helical, in parallel with the NOE data. In some cases, one or both Lys and/or their adjacent residues have $^3J_{HN\alpha} \geq 6$ Hz, probably reflecting an intrinsic behavior of the long unbranched side chain of Lys (*66*) or its low helix propensity (*6*). Similar results have been reported for two longer alanine-lysine peptides in water (*67*, *68*).

Helical residues typically have negative chemical shift index or CSI, the difference between the observed and the random coil $C^{\alpha}H$ $^1H$ chemical shift (refs *52*, *53* and references therein). Figure 3 shows that, in each of the peptides studied here, nearly every residue has a negative CSI in 1 M NaCl and in 40% TFE. Furthermore, N-terminal residues have more negative CSI than those at the C-terminus consistent with the former being more helical in accordance with the NOE and $^3J_{HN\alpha}$ data discussed above. (By contrast, we observe that the $C^{\beta}H$ and the *N*-acetyl $CH_3$ protons move downfield with increasing helix content relative to their random coil values). The helix populations estimated from CD and from $C^{\alpha}H$ $^1H$ chemical shifts (*54*, *55*) show similar overall trends for these peptides (data not shown) being comparable in aqueous 1 M NaCl solutions, but the CD estimates being somewhat greater in 40% TFE. CSI, and thus helix populations estimated from them, are sensitive (*54*, *55*) to electrostatics, ring currents, and other anisotropies, solution conditions, and errors caused by signal overlap in defining the helix length using ($i$, $i + 3$) and ($i$, $i + 4$) NOE data (particularly for alanine-rich peptides such as those studied here), and so were not analyzed using helix-coil theories.

*Tyr-Leu Interactions from NMR Data*. $^1H-^1H$ NOE cross-peaks between the Tyr and Leu side chains are observed in all of the peptides in 1 M NaCl and in 40% TFE (Figure 4) or in 100% TFE but not in 6 M urea (not shown). The absence of these NOEs in 6 M urea shows that they are characteristic only of the helical conformation. Their presence in all peptides in 1 M NaCl or TFE solutions shows that the Tyr and Leu side chains are close enough to interact when spaced ($i$, $i + 4$) or ($i$, $i + 3$) in both the Y−L and L−Y orientations. NOE cross-peaks of the Tyr 2,6 (ortho) or Tyr 3,5 (meta) side-chain protons with the $\delta\delta'$ $CH_3$ protons of Leu are easily identifiable, but those with the Leu $\beta-CH_2$ or the $\gamma$-CH could not be assigned in all the cases because they are weak or are ambiguous as a consequence of signal overlap. 3Y7L and 6L10Y in 1 M NaCl, 40% TFE, or 100% TFE solutions have the Leu $\delta\delta'$-$CH_3$ NOE cross-peak with Tyr 3,5H stronger than that with Tyr 2,6H, indicating that Leu $\delta\delta'$-$CH_3$ and Tyr 3,5H are, on average, closer to one another in these peptides. The reverse is observed for 3Y6L and 7L10Y: the Leu $\delta\delta'$-$CH_3$-Tyr 2,6H NOE cross-peak is stronger and so these two are, on average, closer to one another. Tyr and Leu in the two N- to C-terminal orientations (Y−L or L−Y) are spaced ($i$, $i + 4$) in 3Y7L and 6L10Y, but are spaced ($i$, $i + 3$) in 3Y6L and 7L10Y, indicating that the side-chain NOE cross-peak pattern between the two residues is largely determined by spacing rather than by the relative N- to C-terminal orientation. The similar Tyr and Leu side-chain NOE cross-peak patterns and relative intensities in the presence or absence of TFE show the orientation of the two residues relative to one another and so their side-chain conformational behaviors are not altered by TFE. Information on actual side-chain conformations can, in principle, be provided by structure calculations using NOE

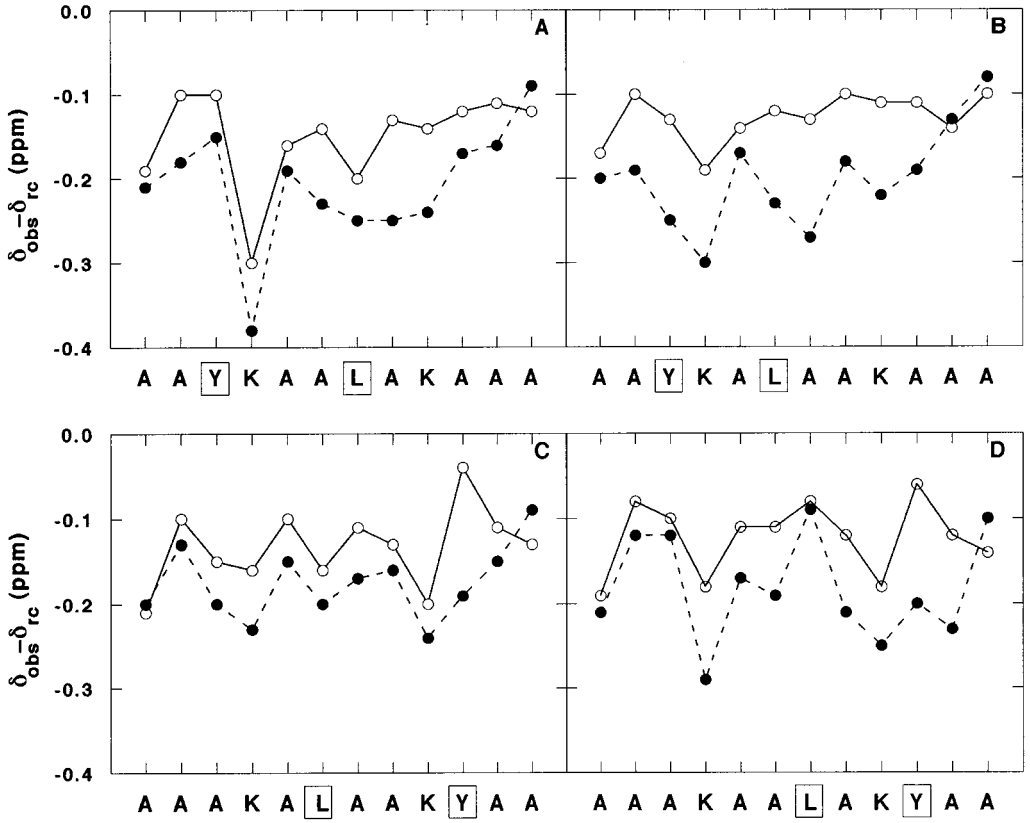


FIGURE 3: CSI values for each residue in the peptides in 1 M NaCl (open circles) and in 40% TFE (filled circles): A, 3Y7L; B, 3Y6L; C, 6L10Y; and D, 7L10Y.

data, but conformational averaging of the NMR parameters and the requirement that the helix content be close to 100% hinder reliable structure calculations for peptides. Only in 40% TFE with the highest helix contents and the greatest number of available medium-range distance constraints (37, 54, 36, and 27, respectively, for 3Y6L, 3Y7L, 6L10Y, and 7L10Y) can any meaningful structure calculations be even attempted. These calculated structures were consistent with the helical conformation of the peptides studied here, but the side chains, in particular those of Leu, are poorly defined. This may be because stereospecific assignments and/or distance constraints for the side chain could not be obtained and so were insufficient for structure calculations (in addition to the other limitations in calculating peptide structures as mentioned above).

The observed Tyr and Leu chemical shifts (in Supporting Information) probably reflect both the differences in helix contents as well as Tyr ring current effects. Consistent with their helical nature, the $C^{\alpha}H$ protons of Tyr and Leu shift upfield relative to their values in 6 M urea or their random coil values (*50, 51*), the shifts being maximum in 40% TFE (Figure 4), but their $C^{\beta}H$ and the Leu $C^{\gamma}H$ protons shift downfield. The Leu $\delta\delta'$ $CH_3$ protons are generally close to their values in 6 M urea or their random coil values, but show somewhat larger upfield shifts for 3Y7L in 1 M NaCl or downfield shifts for 7L10Y in 40% TFE.

*(i, i + 3) and (i, i + 4) Pairs of Tyr and Leu in Proteins.* Table 4 summarizes the results of a search in a database of 315 proteins for ($i$, $i + 3$) and ($i$, $i + 4$) spaced Y−L and L−Y pairs in helices (see Experimental Procedures). It lists the total numbers expected and found for each pair and, of these, the number with side chains in contact, the mean NOE distances between the contacting side chains, and their conformations. In protein α-helices, the ratio of the observed to the expected number of occurrences is 1.3 for the ($i$, $i + 4$) Y−L and the ($i$, $i + 3$) Y−L and L−Y pairs, while it is 1.4 for the ($i$, $i + 4$) L−Y pair. The comparable ratios for the ($i$, $i + 4$) F−M and M−F pairs are 2.4 and 1.4, respectively (*20*−*22*). Of the total found in protein α-helices, Tyr and Leu side chains are in contact in 67% of ($i$, $i + 4$) Y−L pairs, 36% of ($i$, $i + 4$) L−Y pairs, 20% of ($i$, $i + 3$) Y−L pairs, and 23% of ($i$, $i + 3$) L−Y pairs. Thus side-chain contacts occur more often with the ($i$, $i + 4$) spaced pairs than with ($i$, $i + 3$) spaced pairs, being most frequent for the ($i$, $i + 4$) Y−L pair. Since Tyr is closer to the ends in the peptides studied here it could adopt a $3_{10}$-helical conformation like in the end residues of protein helices (*63*−*65*). So we also searched the protein database for ($i$, $i + 3$) and ($i$, $i + 4$) Y−L/L−Y pairs where Tyr is $3_{10}$-helical and all the remaining residues are α-helical. Only four ($i$, $i + 4$) Y−L pairs of which just one showed Y−L side-chain contacts and no others were identified.

Since the most easily and unambiguously identified side-chain $^1H$-$^1H$ NOEs in the peptides studied here are those between the Leu $\delta$ or $\delta'$ $CH_3$ and the Tyr 2,6 or the Tyr 3,5 as discussed earlier (Figure 4), we analyzed the contacting Y−L or L−Y pairs in protein helices for distances and so for possible NOEs between these side-chain protons. The mean and standard deviations for the shortest distances between these side-chain protons are listed in Table 4. They were computed using the shortest distances seen in the protein structures for both of the ortho or both of the meta protons of Tyr from a Leu $\delta$ or $\delta'$ $CH_3$ proton. In protein α-helices with contacting Tyr and Leu pairs, the Leu $\delta$ or

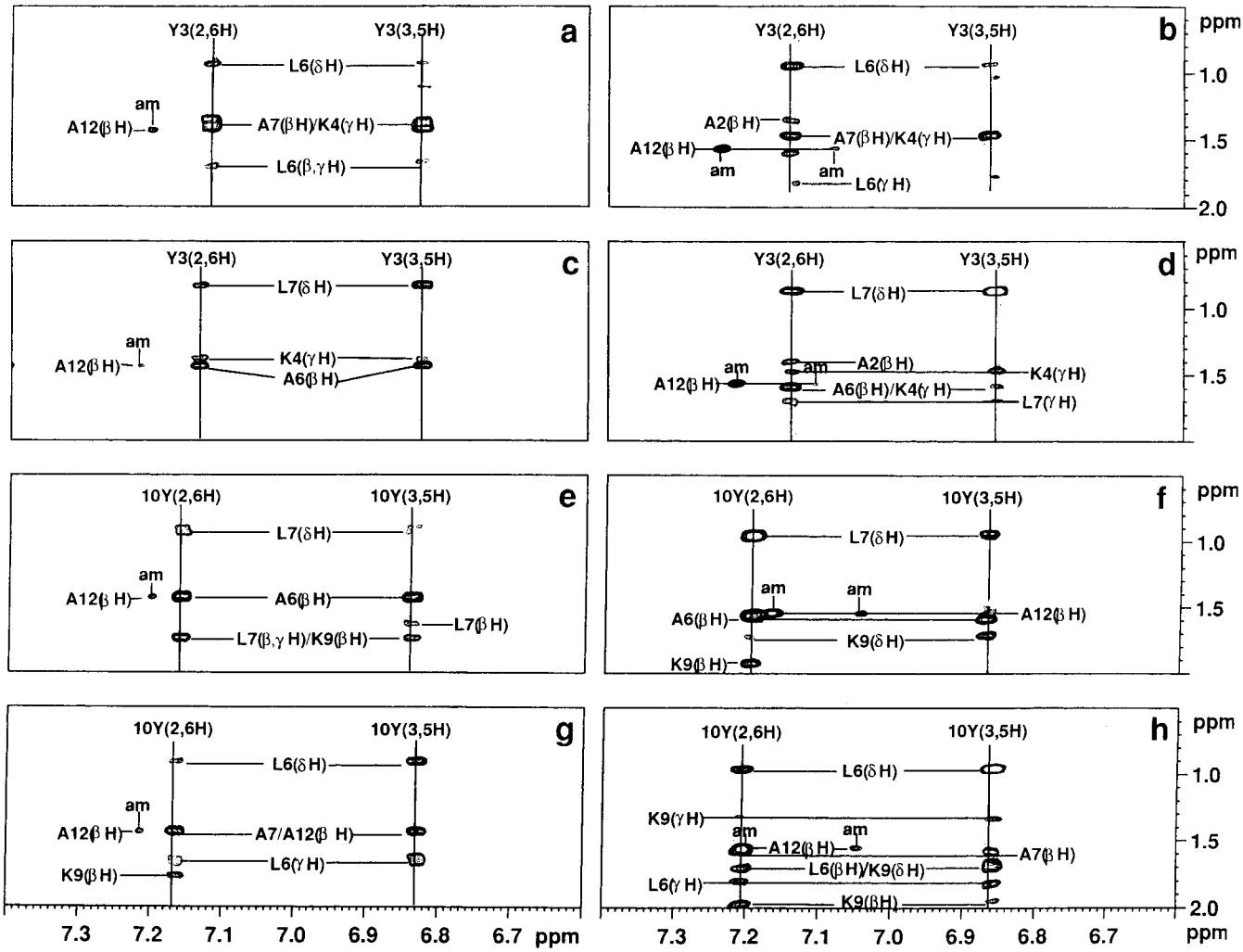


FIGURE 4: Tyr-Leu side-chain NOEs in the peptides in 1 M NaCl (left panel) and in 40% TFE (right panel): a, b, 3Y6L; c, d, 3Y7L; e, f, 7L10Y; and g, h, 6L10Y.

Table 4: ($i$, $i + 3$) and ($i$, $i + 4$) Spaced Tyr and Leu Pairs in Protein Helices[a]

| description | ($i$, $i + 4$) Y−L | ($i$, $i + 3$) YL | ($i$, $i + 4$) LY | ($i$, $i + 3$) LY |
|---|---|---|---|---|
| All YL/LY | 190 | 172 | 200 | 191 |
| helical YL/LY expected | 38 | 43 | 38 | 43 |
| helical YL/LY found | 49 | 56 | 53 | 56 |
| helical YL/LYwith side-chain contact | 33 | 11 | 19 | 13 |
| Y(2,6H)-L($\delta\delta'CH_3$) (Å)[b] | 4.5 ± 0.8 | 3.6 ± 0.7 | 4.1 ± 0.9 | 3.6 ± 0.8 |
| Y(3,5H)-L($\delta\delta'CH_3$) (Å)[b] | 3.5 ± 0.7 | 4.0 ± 0.8 | 3.6 ± 0.8 | 4.7 ± 0.6 |
| $\chi_1$(Y)[c] | 177 ± 26 (100) | −72 ± 9 (64)<br>−170 ± 13 (36) | −70 ± 12 (100) | 170 ± 12 (85) |
| $\chi_2$(Y)[c] | 68 ± 14 (82) | −47 ± 33 (64)<br>49 ± 31 (36) | −59 ± 27 (89) | 74 ± 9 (77) |
| $\chi_1$(L)[c] | −78 ± 22 (73) | −177 ± 16 (55)<br>−72 ± 11 (45) | −77 ± 22 (63)<br>−175 ± 8 (37) | −172 ± 22 (69) |
| $\chi_2$(L)[c] | 179 ± 10 (64)<br>63 ± 9 (36) | 72 ± 13 (55)<br>176 ± 6 (45) | 175 ± 11 (63)<br>58 ± 11 (37) | 64 ± 7 (54)<br>−167 ± 25 (44) |

[a] From a protein database of 315 proteins using WHATIF (*57*, *58*) for the number of occurrences, and NAOMI (*60*) for contacts, angles, and NOE distances (see Experimental Procedures). [b] Mean and standard deviations (SD) for NOE distances. [c] Mean and SD for side-chain dihedral angles ($\chi_1$ and $\chi_2$) computed for the distributions shown in Figure 5 (in parentheses is the percentage of the number of contact pairs used in the computation).

$\delta'$ $CH_3$ is, on average, closer to Tyr 3,5H than to Tyr2, 6H for both of the ($i$, $i + 4$) spaced pairs, but closer to the Tyr2,6H for the ($i$, $i + 3$) spaced pairs, in parallel with the behavior seen in the isolated peptide helices studied here. The mean and standard deviations for the side-chain dihedral angles ($\chi_1$ and $\chi_2$) of Tyr and Leu in each contacting ($i$, $i +$ 4) or ($i$, $i + 3$) pair in protein α-helices are listed in Table 4. Each residue is hardly ever in the rotamer conformation gauche$^-$ or $g^-$ ($\chi_1$ around 60°) in these helices. The preferred Tyr side-chain rotamer conformation is trans or $t$ ($\chi_1$ around 180°) in ($i$, $i + 4$) Y−L and in ($i$, $i + 3$) L-Ypairs, but gauche$^+$ or $g^+$ ($\chi_1$ around −60°) in ($i$, $i + 4$) L−Y pairs. Although in ($i$, $i + 3$) Y−L pairs the Tyr $g^+$ rotamer is preferred a significant number of Tyr $t$ rotamers are also

observed. The preferred Leu rotamer is $g^+$ in both ($i$, $i + 4$) Y−L and L−Y pairs and $t$ in ($i$, $i + 3$) L−Y pairs, while both Leu $t$ and $g^+$ occur with equal frequency in ($i$, $i + 3$) Y−L pairs.

## DISCUSSION

*Alanine-Lysine Peptide Helices.* Alanine-based model peptides are the simplest ones available having negligible, if any, unwanted side-chain interactions and context effects, and are therefore excellent models for investigating both the intrinsic helical propensities of amino acids as well as sequence-specific side-chain interactions of importance in protein folding and stability (*1, 3*−*7*). Studies using this model system have relied almost exclusively on CD and/or NMR measurements of total amide proton exchange kinetics which provide overall helix contents but not information at a residue level. These peptides have eluded crystallization and so are not amenable to X-ray structural analysis. NMR (the only other method which provides a residue level characterization) of alanine-based peptides has been deterred by spectral overlap arising from the presence of several alanines. The overlap problem has been partially addressed using $^{15}$N-labeled alanines at specific positions in the sequence to study amide proton exchange (*61*), or specific $^{13}$C-labeled carbonyls in $^{13}$C chemical shift studies (*69*), but only very recently has a 2D-$^1$H NMR study of an alanine-lysine peptide in water been reported (*68*). The present work addressed the problem of spectral overlap by using shorter peptides whose helix contents are, nevertheless, suitable for quantitative analysis using helix-coil models. Our goal was to examine by 2D-$^1$H NMR the isolated helices formed by these peptides and the conformational basis for the ($i$, $i$ + 4) and ($i$, $i + 3$) Y−L/L−Y interactions present in them in aqueous solutions as well as in TFE and urea solutions. We achieved complete assignment of all the peptide $^1$H NMR signals in aqueous 1 M NaCl or 40% TFE solutions, and then used the presence of a series of (a) NN(i, i+1), αN($i$, $i + 3$), αN($i$, $i + 4$), and αβ($i$, $i + 3$) NOEs; (b) $^3J_{HN\alpha}$ values $< 6.0$; and (c) negative CSI to characterize the helices and the residues involved. These criteria indicated that the overall trends in helix contents parallel CD data, and that the N-terminal residues of the peptides are more helical than the C-terminal ones in both 1 M NaCl and 40% TFE. Similar inferences were made in studies of some longer alanine-lysine peptides in aqueous solutions using amide proton exchange (*61*) or carbonyl $^{13}$C chemical shifts (*69*) or 2D-NMR (*67, 68*), as well as with other N-succinylated or N-acetylated peptides (*70, 71*). Strong medium-range NOEs involving the *N*-acetyl $CH_3$ protons suggest that its conformation is not entirely random as would be expected for complete end-fraying, but that this group participates in helix formation, consistent with its strong N-capping propensity as inferred from the analysis of CD data using models for helix-coil transitions (*6, 27*).

It has been proposed on the basis of ESR studies that alanine-based peptides form $3_{10}$-helices (*72*), although more recent ESR studies have concluded that they are α-helical (*73, 74*). CD cannot distinguish between α- and $3_{10}$-helices. NMR criteria for such a distinction are that α-helices show strong αβ($i$, $i + 3$) and, in particular, αN($i$, $i + 4$) NOEs but no αN(i, i+2) NOEs, whereas $3_{10}$-helices show αN(i, i+2) and weak αβ($i$, $i + 3$) NOEs, but no αN($i$, $i + 4$) NOEs (*47*). The observation of some αN($i$, $i + 4$) and medium to strong αβ($i$, $i + 3$) NOEs in the peptides studied here in 1 M NaCl aqueous solutions suggests that they probably are α-helical, and the significantly large number of these NOEs observed in 40% TFE is strongly indicative of α-helical structure in this solvent. Where observed αN(i, i+2) NOEs are associated with the N- or C-terminal residues as is the case in a longer alanine-based peptide in water (*68*). This may imply a $3_{10}$-helical character (*62*), consistent with the behavior at the ends of protein helices (*64*−*66*). An unambiguous distinction of coexisting α- and $3_{10}$-helices or quantitating their relative populations using NMR data is not straightforward because of effects due to local flexibility, multiple conformations, etc. (*71*), even though this has been attempted recently (*68*). Furthermore, although more sophisticated helix-coil models which consider the presence of both α- and $3_{10}$-helical conformations are now available (*75, 76*), the relevant model parameters have yet to be experimentally determined. For these reasons, only models which consider α-helix to coil transitions (*6, 29*) were used to analyze the peptide data.

*Tyr-Leu Interactions in Isolated Peptides and in Protein Helices.* CD data show that (i) peptides with an ($i$, $i + 4$) Y−L or L−Y pair have a higher helix content than the corresponding ($i$, $i + 3$) pair in aqueous 1 M NaCl solutions, as reported earlier (*18*); (ii) the behavior appears to persist to some extent in 40% TFE solutions, where peptide helix contents are high but where the lower solvent polarity is expected to reduce the contribution of hydrophobic interactions (*6, 31*−*36*); and (iii) helix contents in 6 M urea are negligible. NMR data in the different solution conditions reflect the relative helix contents in a manner consistent with CD data. In all the four peptides containing ($i$, $i + 3$) or ($i$, $i + 4$) Y−L or L−Y pairs, NOE cross-peaks between the Tyr and Leu side chains are observed in 1 M NaCl, and in 40% or 100% TFE solutions but not in 6 M urea. Thus in ($i$, $i + 3$) and ($i$, $i + 4$) Y−L/L-Ypairs, Tyr and Leu are close enough to one another to interact in 1 M NaCl, and in 40% TFE and even in 100% TFE solutions, the latter are reported to have lower helix contents (from CD) than in 40% TFE but greater than in 100% water (*32*). These Tyr-Leu interactions are not observed in 6 M urea (where CD and NMR data indicate absence of any regular structure), unlike in some peptide fragments of proteins where nonpolar residues especially aromatic ones such as Tyr, appear to interact in the unstructured state to form hydrophobic clusters (*77*−*80*). It may be noted that the presence of these side-chain NOEs, while indicating that the two residues are close enough to interact, gives no indication of the relative strengths of these interactions. This information cannot be inferred from comparisons of the absolute NOE cross-peak intensities because of differences in helix contents and conformational averaging, as well as in solvent and peptide concentrations. The patterns and relative intensities of the NOE cross-peaks can, however, be compared. The same pattern of NOE cross-peak intensities between the Tyr aromatic and the Leu $\delta\delta'$-$CH_3$ protons observed for a given peptide in 1 M NaCl, 40% TFE and in 100% TFE solutions suggests that the side-chain conformational behavior for a specific Y−L or L−Y pair in 1 M NaCl is not altered by TFE. On the basis of the relative NOE cross-peak intensities it appears that the Leu $\delta\delta'$-$CH_3$ is closer, on average, to the

Table 5: ($i$, $i + 3$) and ($i$, $i + 4$) Nonpolar/Aromatic Interactions in Peptide Helices

| X−Y pair | ($i$, $i + 4$) $\Delta G_{X-Y}$(kcal mol$^{-1}$) | | | ($i$, $i + 3$) $\Delta G_{X-Y}$(kcal mol$^{-1}$) | | |
|---|---|---|---|---|---|---|
| | mL-R | AGADIR | MC[a] | mL-R | AGADIR | MC[a] |
| Y−L[b] | −0.79 ± 0.10 | −0.68 ± 0.08 | −0.33 | −0.24 ± 0.17 | −0.32 ± 0.12 | −0.18 |
| L−Y[b] | −1.00 ± 0.09 | −1.10 ± 0.10 | −0.42 | −0.62 ± 0.11 | −0.57 ± 0.12 | −0.27 |
| C−M | −0.75 ± 0.09[c] | −0.65 ± 0.15[d] | −0.19 | na[e] | na[e] | −0.26 |
| M−C | −0.54 ± 0.06[c] | −0.20 ± 0.20[d] | −0.32 | na[e] | na[e] | −0.20 |
| W−H[f] | −1.0 ± 0.20 | −0.80 ± 0.10 | −0.22 | na[e] | −0.2 ± 0.5 | −0.37 |
| H−W[f] | na | (0.20 ± 1.5) | −0.40 | na[e] | −(0.1 ± 0.5) | 0.28 |
| C−L[g] | −0.47 ± 0.12 | −0.20 ± 0.10 | −0.30 | 0.00 ± 0.10 | 0.00 ± 0.10 | −0.18 |
| L−C[g] | −0.56 ± 0.13 | −0.60 ± 0.10 | −0.24 | −0.10 ± 0.15 | 0.00 ± 0.10 | −0.26 |
| V−L[g] | −0.85 ± 0.19 | −0.58 ± 0.10 | −0.31 | −0.33 ± 0.09 | −0.22 ± 0.10 | −0.05 |
| L−V[g] | −0.99 ± 0.18 | −0.92 ± 0.10 | −0.06 | −0.32 ± 0.12 | −0.15 ± 0.10 | −0.08 |
| I−L[g] | −0.83 ± 0.17 | −0.68 ± 0.12 | −0.35 | −0.25 ± 0.11 | −0.30 ± 0.10 | −0.13 |
| L−I[g] | ∼1.60 | −1.5 ± 0.25 | −0.09 | −0.66 ± 0.17 | −0.49 ± 0.13 | −0.12 |
| L−L[g] | −0.59 ± 0.21 | −0.60 ± 0.13 | −0.02 | −0.29 ± 0.11 | −0.35 ± 0.12 | −0.02 |

[a] See ref *23*. [b] NaCl (1 M), pH 3.0 (1 mM sodium phosphate/citrate/borate), 2 °C (this study). [c] NaCl (10 mM), pH 7.0 (5 mM sodium phosphate), 0 °C (*20*). [d] No salt, pH 3.0, 5 °C, (*21*). [e] Not available. [c] NaCl (25 mM), pH 5.0 (1 mM sodium phosphate/citrate/borate), 2 °C (*24*). [g] Analyzed cor data in 1 M NaCl, pH 7.0 (1 mM sodium phosphate/citrate/borate), 0 °C (*19*).

Tyr 3,5H (meta) protons than to the Tyr 2,6H (ortho) protons in ($i$, $i + 4$) Y−L or L−Y pairs, but closer to the Tyr 2,6H than to Tyr 3,5H protons in the ($i$, $i + 3$) Y−L and L−Y pairs. This same behavior is seen in protein α-helices containing ($i$, $i + 3$) or ($i$, $i + 4$) Y−L or L−Y pairs where the Tyr and Leu side chains are in contact, so that it is reasonable to infer that the side-chain conformations for a given Tyr and Leu pair in the peptides are similar to that pair when in contact in protein helices. Therefore, the preferred Tyr and Leu conformations are, respectively, $t$ and $g^+$ in ($i$, $i + 4$) Y−L pairs, $g^+$and $g^+$ in ($i$, $i + 4$) L−Y pairs, and $t$ and $t$ in ($i$, $i + 3$) L−Y pairs, while $t$ and $g^+$ are more or less equally likely for Tyr and Leu in ($i$, $i + 3$) Y−L pairs (Table 4). Calculations indicate that in a helix the $t$ and $g^+$ rotamers of Leu are, within error, energetically equivalent, but for Tyr the $t$ is about 0.5 kcal mol$^{-1}$ more favorable (*81*). Thus Tyr adopts the more favorable $t$ rotamer conformation in ($i$, $i + 4$) Y−L and ($i$, $i + 3$) L−Y pairs and the less favorable one ($g^+$) in ($i$, $i + 4$) L−Y pairs, thereby explaining, at least partly, the relative helix-stabilizing tendencies among these pairs.

($i$, + 3) and ($i$, $i + 4$) Y−L and L−Y pairs have nonzero, helix-stabilizing interaction energies as estimated by analyzing helix contents using the modified Lifson-Roig (*6*) and/or AGADIR (*29*) model helix-coil transitions. In 40% TFE the lower limit values for the interaction energies are smaller than those in 1 M NaCl solutions but not 0, at least for the ($i$, $i + 4$) pairs. TFE thus appears to decrease the contribution of hydrophobic interactions, and this has been also reported for electrostatic interactions (*36*). In 1 M NaCl solutions, the Y−L/L−Y interaction energies are comparable to or exceed those for some of the other nonpolar residue pairs in isolated peptides (Table 5), the latter being those reported elsewhere (*20*, *21*, *24*), or are lower limit values calculated using CD helix content data uncorrected for aromatic contributions from reference (*19*). Both mL-R and AGADIR yield estimates for the interaction energies for these nonpolar pairs which are similar but not identical, probably because of the differences in the two formalisms, in some of the parameter values (discussed in refs *20*, *29*), and also, in some cases, in the solution conditions used. These interaction energies obtained by analysis of experimental data are, in almost all cases, greater than theoretical estimates (Table 5) obtained using an exhaustive conformational search procedure in a model polyalanine α-helix (*23*). It has been proposed that the discrepancy may be the consequence of possible interactions between the hydrophobic, methylene portion of a lysine side chain with one of the residues of the nonpolar pair (*23*). Our examination by CD of the helix contents of a set of peptides with and without ($i$, $i + 3$) L−K or K−L pairs shows essentially no interactions between Lys and Leu spaced ($i$, $i + 3$) which affect helix formation. This appears to be consistent with other studies which also suggested little or no measurable interactions between flexible straight-chain amino acids (*7*, *19*). Interaction between two side chains requires them to be in a fixed conformation, and the resulting loss in side-chain conformational entropy is unfavorable. This would be particularly unfavorable for residues such as Lys whose side chains are flexible and less restricted in an α-helix. $^1$H NMR studies of "template-nucleated" (covalently fixed first helical turn) alanine-rich peptides containing a single Lys and specifically deuterated alanines indicated NOEs, indicative of interactions, between the Lys side chain and the peptide backbone (*82*). The presence of such NOEs could not be verified for the peptides in this study because of considerable overlap of these side-chain resonances. However, for reasons that remain unclear, the relative helix-forming tendencies of Ala as well as Lys and its analogues with successively fewer side-chain methylenes in this template-nucleated peptide system (*82*) differ from those in alanine-lysine peptides of the type used in this study (*6*, *83*).

($i$, $i + 4$) and ($i$, $i + 3$) Y−L and L−Y pairs in protein α-helices are somewhat more frequent than expected. It has been suggested that the occurrence of a specific pair of amino acids more frequently than expected indicates the existence of a favorable interaction between their side chains, the free energy of which is related to the ratio of the observed to the expected frequencies of occurrence by the Boltzmann equation (*84*). Such an analysis would mean that all ($i$, $i + 3$) and ($i$, $i + 4$) pairs of Tyr and Leu which occur in protein helices with similar frequencies would have nearly identical, helix stabilizing interaction energies, an inference contrary to the greater helix-stabilization by the ($i$, $i + 4$) pairs relative to the ($i$, $i + 3$) pairs observed in the peptides studied here. Contacts between the Tyr and Leu side chains in protein helices, however, are more frequently observed for the ($i$, $i + 4$) pairs than for the ($i$, $i + 3$) pairs, although their rank

order of contact frequencies does not correspond exactly to the rank order of the helix-stabilizing tendencies observed in peptides for the different Tyr and Leu pairs. The frequency of occurrence in protein helices of a specific type of Y−L or L−Y pair is, of course, determined not only by interactions between their side chains, but also by competing interactions of Tyr and/or Leu with other ($i$, $i + 3$) or ($i$, $i + 4$) spaced nonpolar residues (*18*, *19*) commonly observed in protein helices, and by the energetically stronger tertiary packing interactions. Y−L, L−Y, and other nonpolar interactions must, nevertheless, be important in the early stages of protein folding in forming and stabilizing helices. The free energies determined for these interactions, together with others such as hydrogen bonding and salt bridges, and the intrinsic helix propensities would also enable the helix contents of isolated peptides and unfolded proteins to be predicted and to be used in rationalizing the apparent context dependence of helix-forming tendencies.

## ACKNOWLEDGMENT

S.P. initiated this study in the laboratory of Professor R. L. Baldwin (Stanford University) and thanks him for his support. We are indebted to Dr. Jorge Santoro for help in the calculations of coupling constants, to Dr. Grant Langdon for the use of the program NAOMI, to Drs. Javier Sancho and Juan Fernández-Recio (University of Zaragoza) for help with the AGADIR calculations, to Domingo García for structure calculations, and to Cristina López and Apolo Gómez for assistance. We acknowledge the use of the mass spectrometer, CD, and HPLC facilities in the Protein Chemistry Division, CIB-Madrid.

## SUPPORTING INFORMATION AVAILABLE

Tables showing the proton chemical shifts for peptides 3Y7L, 3Y6L, 6L10Y, and 7L10Y in 1 M NaCl (Tables 1A−D, four tables), in 40% TFE (Tables 2A−D, four tables), and in 6 M urea (Tables 3A−D, four tables) (10 pages). Ordering information is given on any current masthead page.

## REFERENCES

1. Baldwin, R. L. (1995) *Biophys. Chem. 55*, 127−135.
2. Wójcik, J., Altmann, K.-H., and Scheraga, H. A. (1990) *Biopolymers 30*, 121−134.
3. Marqusee, S., Robbins, V., and Baldwin, R. L. (1989) *Proc. Natl. Acad. Sci. U.S.A. 86*, 5286−5290.
4. Padmanabhan, S., Marqusee, S., Ridgeway, T., Laue, T. M., and Baldwin, R. L. (1990) *Nature 344*, 268−270.
5. Chakrabartty, A., Kortemme, T., and Baldwin, R. L. (1994) *Protein Sci. 3*, 843−852.
6. Rohl, C. A., Chakrabartty, A., and Baldwin, R. L. (1996) *Protein Sci. 5*, 2623−2637.
7. Padmanabhan, S., York, E. J., Gera, L., Stewart, J. M., and Baldwin, R. L. (1994) *Biochemistry 33*, 8604−8608.
8. Myers, J. K., Pace, C. N., and Scholtz, J. M. (1997) *Proc. Natl. Acad. Sci. U.S.A. 94*, 2833−2837.
9. Regan, L. (1997) *Proc. Natl. Acad. Sci. U.S.A. 94*, 2796−2797.
10. Yang, J., Spek, E. J., Gong, Y., Zhou, H., and Kallenbach, N. R. (1997) *Protein Sci. 6*, 1264−1272.
11. Muñoz, V., and Serrano, L. (1996) *Folding Des. 1*, R71−77.
12. Doyle, R., Simons, K., Qian, H., and Baker, D. (1997) *Proteins: Struct., Funct., Genet. 29*, 282−291.
13. Lotan, N., Yaron, A., and Berger, A. (1966) *Biopolymers 4*, 365−368.
14. Richards, F. M., and Richmond, T. (1978) in *Molecular Interactions and Activity in Proteins* (Wolstenholme, G. E., Ed.) pp 23−45, CIBA Found. Symp. 60, Amsterdam Excerpta Medica.
15. Baldwin, R. L. (1989) *Trends Biochem Sci. 14*, 291−294.
16. Dill, K. A. (1990) *Biochemistry 29*, 7133−7155.
17. Dill, K. A., Fiebig, K. M., and Chan, H. S. (1993) *Proc. Natl. Acad. Sci. U.S.A. 90*, 1942−1946.
18. Padmanabhan, S., and Baldwin, R. L. (1994) *J. Mol. Biol. 241*, 706−713.
19. Padmanabhan, S., and Baldwin, R. L. (1994) *Protein Sci. 3*, 1992−1997.
20. Stapely, B. J., Rohl, C. A., and Doig, A. J. (1995) *Protein Sci. 4*, 2383−2391.
21. Viguera, A. R., and Serrano, L. (1995) *Biochemistry 34*, 8771−8779.
22. Klingler, T. M., and Brutlag, D. L. (1995) *Protein Sci. 3*, 1847−1857.
23. Creamer, T. P., and Rose, G. D. (1995) *Protein Sci. 4*, 1305−1314.
24. Fernandez-Recio, J., Vazquez, A., Civera, C., Sevilla, P., and Sancho, J. (1997) *J. Mol. Biol. 267*, 184−197.
25. Lifson, L., and Roig, A. (1961) *J. Chem. Phys. 34*, 1963−1974.
26. Zimm, B. H., and Bragg, J. K. (1959) *J. Chem. Phys. 31*, 526−535.
27. Doig, A., Chakrabartty, A., Klingler, T., and Baldwin, R. L. (1993) *Biochemistry 33*, 3396−3403.
28. Muñoz, V., and Serrano, L. (1994) *Nat. Struct. Biol. 1*, 399−409.
29. Muñoz, V., and Serrano, L. (1997) *Biopolymers 41*, 495−509.
30. Shalongo, W., and Stellwagen, E. (1995) *Protein Sci. 4*, 1161−1166.
31. Jasanoff, A., and Fersht, A. (1994) *Biochemistry 33*, 2129−2135.
32. Albert, J. S., and Hamilton, A. D. (1995) *Biochemistry 34*, 984−990.
33. Cammers-Goodwin, A., Allen, T. J., Oslick, S. L., McClure, K. F., Lee, J. H., and Kemp, D. S. (1996) *J. Am. Chem. Soc. 118*, 3082−3090.
34. Hirota, N., Mizuno, K., and Goto, Y. (1998) *J. Mol. Biol. 275*, 365−378.
35. Luo, P., and Baldwin, R. L. (1997) *Biochemistry 36*, 8413−8421.
36. Myers, J. K., Pace, C. N., and Scholtz, J. M. (1998) *Protein Sci. 7*, 383−388.
37. Houghten, R. A. (1985) *Proc. Natl. Acad. Sci. U.S.A. 82*, 5131−5135.
38. Brandts, J. F., and Kaplan, K. J. (1973) *Biochemistry 12*, 2011−2024.
39. Chen, G. C., and Yang, J. T. (1977) *Anal. Lett. 10*, 1195−1207.
40. Chakrabartty, A., Kortemme, T., Padmanabhan, S., and Baldwin, R. L. (1993) *Biochemistry 32*, 5560−5565.
41. Marion, D., and Wüthrich, K. (1983) *Biochem. Biophys. Res. Commun. 113*, 967−974.
42. Aue, W. P., Bartholdi, E., and Ernst, R. R. (1976) *J. Chem. Phys. 64*, 2229−2246.
43. Kumar, A., Ernst, R. R., and Wüthrich, K. (1980) *Biochem. Biophys. Res. Commun. 95*, 1−6.
44. Bothner-By, A. A., Stephens, R. L., Lee, J. M., Warren, C. D., and Jeanloz, R. W. (1984) *J. Am. Chem. Soc. 106*, 811−813.
45. Rance, M., Sorensen, O. W., Bodenhausen, G., Wagner, G., Ernst, R. R., and Wüthrich, K. (1983) *Biochem. Biophys. Res. Commun. 117*, 479−485.
46. Bax, A., and Davis, D. G. (1985) *J. Magn. Reson. 65*, 355−360.
47. Wüthrich, K. (1986) *NMR of proteins and nucleic acids*, J. Wiley and Sons, Inc., New York.
48. Stonehouse, J., and Keeler, J. (1995) *J. Magn. Reson., Ser. A 112*, 43−57.

49. Kim, Y., and Prestegard, J. H. (1989) *J. Magn. Reson. 84*, 9−13.
50. Merutka, G., Morikis, D., Brüschweiler, R., and Wright, P. E. (1995) *J. Biomol. NMR 5*, 14−24.
51. Wishart, D. S., Bigam, C. G., Holm, A., Hodges, R. S., and Sykes, B. D. (1995) *J. Biomol. NMR. 5*, 67−81.
52. Wishart, D. S., Sykes, B. D., and Richards, F. M. (1991) *J. Mol. Biol. 222*, 311−333.
53. Wishart, D. S., Sykes, B. D., and Richards, F. M. (1992) *Biochemistry 31*, 1647−1651.
54. Jiménez, M. A., Bruix, M., González, C., Blanco, F. J., Nieto, J. L., Herranz, J., and Rico, M. (1993) *Eur. J. Biochem. 207*, 39−49.
55. Rizo, J., Blanco, F. J., Kobe, B., Bruch, M. D., and Gierach, L. M. (1993) *Biochemistry 32*, 4881−4894.
56. Güntert, P., Braun, W., and Wüthrich, K. (1991) *J. Mol. Biol. 217*, 517−530.
57. Vriend, G. (1990) *J. Mol. Graphics 8*, 52−56.
58. Vriend, G., Sander, C., and Stouten, P. F. W. (1994) *Protein Eng. 7*, 23−29.
59. Kabsch, W., and Sander, C. (1983) *Biopolymers 22*, 2577−2637.
60. Brocklehurst, S. M., and Perham, R. N. (1993) *Protein Sci. 2*, 626−639.
61. Rohl, C. A., and Baldwin, R. L. (1994) *Biochemistry 33*, 7760−7767.
62. Dyson, H. J., and Wright, P. E. (1991) *Annu. Rev. Biophys. Biophys. Chem. 20*, 519−538.
63. Némethy, G., Phillips, D. C., Leach, S. J., and Scheraga, H. A. (1967) *Nature 214*, 363−365.
64. Baker, E. N., and Hubbard, R. E. (1984) *Prog. Biophys. Mol. Biol. 44*, 97−179.
65. Barlow, D. J., and Thornton, J. M. (1988) *J. Mol. Biol. 201*, 601−619.
66. Smith, L. J., Bolin, K. A., Schwalbe, H., MacArthur, M. W., Thornton, J. M., and Dobson, C. M. (1996) *J. Mol. Biol. 255*, 494−506.
67. Millhauser, G. L., Stenland, C. J., Bolin, K. A., and van de Ven, F. J. M. (1996) *J. Biomol. NMR 7*, 331−334.
68. Millhauser, G. L., Stenland, C. J., Bolin, K. A., and van de Ven, F. J. M. (1997) *J. Mol. Biol. 267*, 963−974.
69. Shalongo, W., Dugad, L., and Stellwagen, E. (1994) *J. Am. Chem. Soc. 116*, 8288−8293.
70. Liff, M. I., Lyu, P. C., and Kallenbach, N. R. (1991) *J. Am. Chem. Soc. 113*, 1014−1019.
71. Merutka, G., Morikis, D., Brüschweiler, R., and Wright, P. E. (1993) *Biochemistry 32*, 13089−13097.
72. Miick, S. M., Martinez, G. V., Fiori, W. R., Todd, A. P., and Millhauser, G. L. (1992) *Nature 359*, 653−655.
73. Rabenstein, M. D., and Shin, Y. K. (1995) *Proc. Natl. Acad. Sci. U.S.A. 92*, 8239−8243.
74. Smythe, M. L., Nakaie, C. R., and Marshall, G. R. (1995) *J. Am. Chem. Soc. 117*, 10555−10562.
75. Sheinerman, F. B., and Brooks, C. L. (1995) *J. Am. Chem. Soc. 117*, 10098−10103.
76. Rohl, C. A., and Doig, A. J. (1996) *Protein Sci. 5*, 1687−1696.
77. Neri, D., Billeter, M., Wider, G., and Wüthrich, K. (1992) *Science 257*, 155−1563.
78. Dyson, H. J., Merutka, G., Waltho, J. P., Lerner, R. A., and Wright, P. E. (1992) *J. Mol. Biol. 226*, 795−817.
79. Kemmink, J., and Creighton, T. E. (1993) *J. Mol. Biol. 234*, 861−878.
80. Lumb, K. J., and Kim, P. (1994) *J. Mol. Biol. 236*, 412−420.
81. Stapely, B. J., and Doig, A. J. (1997) *J. Mol. Biol. 272*, 456−464.
82. Groebke, K., Renold, P., Tsang, K. Y., Allen, T. J., McClure, K. F., and Kemp, D. S. (1996) *Proc. Natl. Acad. Sci. U.S.A. 93*, 2045−2049.
83. Padmanabhan, S., York, E. J., Stewart, J. M., and Baldwin, R. L. (1996) *J. Mol. Biol. 257*, 726−734.
84. Sippl, M. (1990) *J. Mol. Biol. 213*, 859−883.

BI9813678